Journal of Molecular Structure 1189 (2019) 265–271

Contents lists available at ScienceDirect

Journal of Molecular Structure

journal homepage: http://www.elsevier.com/locate/molstruc

Crystallization of ionic liquid [EMIM][NO_3] under extreme conditions

Jie Wu [a], Xuerui Cheng [a, **], Mingyang Wu [a], Haining Li [a], Xiang Zhu [a], Zheng Wang [a], Chaosheng Yuan [a], Kun Yang [a], Lei Su [b, *]

[a] School of Physics and Electronic Engineering, Zhengzhou University of Light Industry, Zhengzhou, Henan, 450002, China
[b] Center for High Pressure Science and Technology Advanced Research, Beijing, 100094, China

ARTICLE INFO

Article history:
Received 10 February 2019
Received in revised form
10 April 2019
Accepted 11 April 2019
Available online 12 April 2019

Keywords:
Ionic liquid
Phase transition
Low temperature
High pressure
Conformer

ABSTRACT

Phase behavior of the ionic liquid 1-Ethyl-3-Methylimidazolium Nitrate [EMIM][NO_3] has been investigated by using differential scanning calorimetry (DSC) and Raman spectroscopy. From the DSC results, it can be confirmed that [EMIM][NO_3] crystallizes at Tc = 251 K and melts at T_m = 289 K with the cooling or heating rate of 10 K/min. Raman results demonstrate that the cation [EMIM] has a nonplanar-planar equilibrium of the ethyl group in the liquid state, while its solid structure obtained by cooling is formed with planar conformation. The high-pressure Raman spectra reveals that [EMIM][NO_3] undergoes liquid to solid I phase transition at about 0.9 GPa and then transforms into solid II at about 2.2 GPa upon compression. Notably, another new phase transition is observed during decompression process. The nonplanar conformer is predominant under high pressures. In addition, Raman spectra of [EMIM][NO_3] of the different phases are compared in detail, and the results show that the structure of the solid state at low temperature is different from these of the high pressure states.

1. Introduction

Over the past decades, ionic liquids (ILs) have been attracting significant interest owing to their unique characteristics. And ionic liquids are also called “designer solvents” and fulfill a wide range of specific needs [1]. Most of them are composed of sterically mismatched ions with low charge density, and those larger and less symmetric ions are likely to adopt multiple conformations not only lead to a large entropic contribution in the solidification process but also result in packing hindrance and inhibiting crystallization. Therefore, they often form vitrified state below the melting temperature T_m and show a complex phase behavior [2–4].

Phase behavior is a fundamental physical chemistry issue for potential application, thus the research on phase transition of ionic liquids is essential in industrial processes. Firstly, temperature is an important thermodynamic parameter which affects the structure and properties of materials. Considerable amounts of literature have reported the phase transition of ionic liquids at low temperature [5–9]. For some ionic liquids, the formation of solid phase is dependent on the changing rate of temperature. Even only glassy state was obtained at low temperature. Besides temperature, pressure also affects the structure and chemical stability by changing the intermolecular and intramolecular distances but no thermal effects on dynamics. Therefore, pressure is considered as another effective approach to discover novel properties or phase transition of materials [10,11]. In recent years, some researches have focused on the phase behavior and conformational changes of ionic liquids under high pressure [11–16]. Although both cooling and compression can cause phase transitions of ionic liquids, crystallization of ionic liquids under different extreme conditions are often different. For example, 1-butyl-1-methylpyrrolidinium bis(trifluoromethanesulfonyl)imide (PYR_{14}-TFSI) displays two low-temperature crystalline phases, but only one glassy phase in the high-pressure regime [11]. Similar with PYR_{14}-TFSI, *N*-butyl-trimethylammonium Bis(trifluoromethanesulfonyl)imide ([N_{1114}][NTf_2]) can crystallize on cooling, but vitrify under high pressure [12]. As one important imidazolium-based ionic liquid, 1-Butyl-3-Methylimidazolium Hexafluorophosphate ([BMIM][PF_6]) is easily crystallized upon compression (0.3 GPa), and further compression leads to the discovery of another crystal structure above 1.0 GPa, which has no relation with the low-temperature crystals [14,15].

The imidazolium-based ionic liquid, 1-Ethyl-3-Methylimidazolium Nitrate ([EMIM][NO_3]), is an interesting substitute for industrial applications, because it contains no fluoride to

* Corresponding author.
** Corresponding author.
E-mail addresses: xuerui461@163.com (X. Cheng), zz_sulei@163.com (L. Su).

https://doi.org/10.1016/j.molstruc.2019.04.054
0022-2860/

avoid the release of toxic and corrosive hydrogen fluoride into the environment [17]. The phase behavior of [EMIM][NO_3] under high pressure has been studied, and three different crystalline phases has been observed during compression up to 8.6 GPa [18,19]. Besides compression, new structure crystallization has also been reported for some ionic liquids during decompression [20,21]. However, up to now, there are no reports on the observation of new phase of [EMIM][NO_3] during decompression process. In order to further investigate the structure and phase transition of such kind of material under extreme conditions, in this work, crystallization of ionic liquid [EMIM][NO_3] has been investigated under extreme conditions from 180 to 320 K or under high pressure up to 4.5 GPa in detail. Our approach is to investigate how the temperature and pressure lead to the new polymorph and to compare with the crystallization phase induced by high pressure and low temperature.

2. Experimental section

[EMIM][NO_3], (Lanzhou Institute of Chemical Physics, Chinese Academy of Science), with purity above 99.5%, was used as the starting material without further purification. The molecular weight is 173.08 g/mol. The sample was kept under high vacuum at a moderate temperature (323.15 K) for several days to reduce the moisture content and volatile compounds to negligible values and then appeared a transparent liquid state. The water content was doubly checked to be less than 150 ppm which was determined by Karl Fischer titration method.

Differential scanning calorimetry (DSC) was measured with DSC 250 instrument under an inert nitrogen flux, and approximately 10 mg of samples was sealed in an aluminum pan. In order to avoid possible contamination, the sample [EMIM][NO_3] was loaded into a capillary with 0.33 mm diameter which was sealed under vacuum. The low temperature Raman spectra were acquired by using the Linkam THMS600 Heating and Freezing Stage (Japan Hightech), the cooling rate was 10 K/min.

The high-pressure equipment used in this experiment was a diamond anvil cell (DAC), with two diamonds of 0.8 mm culet size that produced high. The sample was loaded in a 0.1 mm diameter which was drilled in the center of a 0.09 mm thick preindented T301 stainless steel gasket. Pressure calibrations were calculated with the shift of the ruby R1 fluorescence line without pressure medium with a precision of 0.02 GPa [22]. The Raman experiments were performed by a Renishaw inVia Raman microscope (Renishaw, United Kingdom) with 532 nm excitation line. Raman spectra were collected in a backscattering geometry with a 2400 gr/mm holographic grating, and the slit width was selected as 65 μm corresponding to a resolution of ca. 0.5 cm^{-1}. The sample image can be collected through an achromatic lens and then focused onto a CCD detector for visually monitoring during experiments. The samples were held at each pressure and temperature for 20 min to establish equilibrium, and then the data was collected. All of the collected Raman spectra were fitted with Gaussian-Lorentzian mixing functions by using the WIRE 3.3 software (Renishaw, United Kingdom) for analyzing the spectral data.

3. Results and discussion

Differential scanning calorimeter (DSC) is performed to explore the phase behavior of [EMIM][NO_3] at low temperatures. Fig. 1 shows DSC thermogram of [EMIM][NO_3] in the range 190–320 K. The sample is heated to 320 K and hold for a period of time to remove crystal nuclei eventually appeared in the liquid phase. Then it is cooled to 190 K and heated to 320 K with the rate of 10 K/min. A

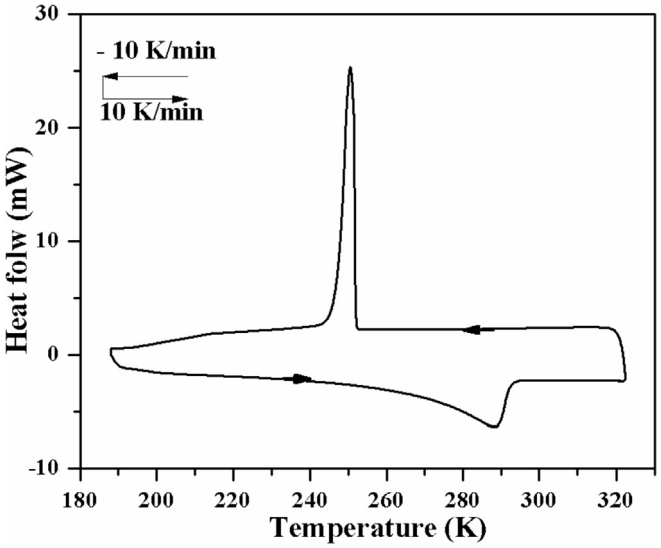

Fig. 1. Differential scanning calorimetry (DSC) thermogram of [EMIM][NO_3] with the cooling and heating rate of 10 K/min.

sharp exothermic peak is observed at approximately 251 K during cooling. This peak is ascribed to the liquid to crystal transition. Crystallization occurs during cooling and no other complex thermal histories are detected, which mean that this sample is not as easily vitrified as other ionic liquids. Upon heating, the sample begins to endothermic slowly at about 238 K, showing a slope of the DSC curve. Then endothermic reaches its maximum, with a broad endothermic peak at about 289 K. The peak 289 K of the melting curve for ionic liquid [EMIM][NO_3] is defined as the melting temperature. This temperature is very different from the reported melting point, which is related to water content and temperature changing rates [23]. Dependence on the local melting, the melting of ILs is usually accompanied with pre-melting phenomenon. The complex thermal behavior has been reported in other ionic liquids, such as butyltrimethylammonium bis(trifluoromethylsulfonyl) imide ([$C_4C_1C_1C_1N$][Tf_2N]), there is a broad premelting peak preceding the sharp melting, defined as rhythmic melting [24]. Meanwhile like [EMIM][NO_3], the melting process of 1-ethyl-3-methylimidazolium hydrogen sulfate ([C_2C_1im][HSO_4]) also covers an extended temperature range, and this mechanism of melting is characterized as continuous melting [9]. This thermal phenomenon is relevant to phase transitions and conformational changes caused by the formation and collapse of polar and nonpolar regions [9,24].

Raman spectra provide the insights on the nature of ionic interactions, the role of anion-cation hydrogen bonds and molecular conformations. In consequence, it is a powerful instrument to reveal the structural modifications accompanying phase transitions and conformational changes. Fig. 2 displays the Raman spectra of [EMIM][NO_3] at different temperature under ambient pressures. The assignments of vibrational bands are based on reported theoretical studies [16,25,26]. Initially, there is no significant change in the profile and intensity of the Raman spectrum. When the temperature decreases to 240 K, the Raman bands become sharper, and some new characteristic bands appear dramatically (marked as an asterisk* in Fig. 2). Especially in the 2800–3200 cm^{-1} range which has been used as a useful probe to reflect structural changes, Raman spectra exhibits significant changes. C–H stretching of the alkyl chains at 2890 cm^{-1} and the imidazolium ring at 3164 cm^{-1} split into two peaks respectively. And a sharp peak appears at 3055 cm^{-1}. Combined with the previous result of DSC, it can be drawn that [EMIM][NO_3] experiences a liquid-solid phase

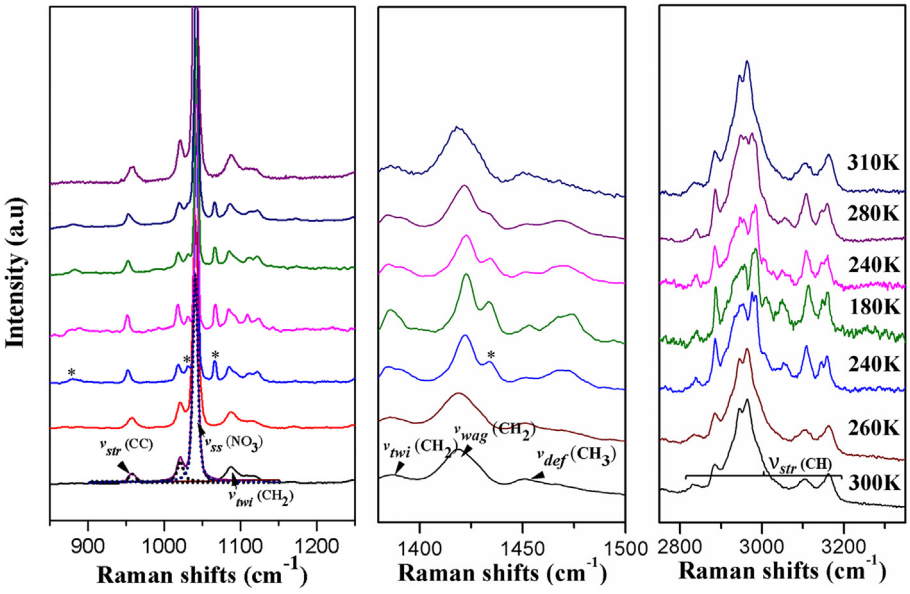

Fig. 2. Raman spectra of [EMIM][NO_3] at different temperatures. The asterisks (*) represent new Raman peaks.

transition at about 240 K upon cooling. As the temperature decreases to 180 K and increase to 290 K, there are no obvious changes in Raman spectrum. When the sample is reheated to 310 K, Raman spectrum restore to the shape of initial liquid state.

To characterize phase transitions more clearly, temperature dependent evolution of Raman frequencies and full width at half maximum (FWHM) values for some selected modes are presented in Fig. 3. There are two discontinuous changes observed at around 240 K upon cooling and at around 300 K upon heating respectively, which further supports the phase transitions previous induced by temperature. In general, once liquid-solid phase transition occurs, unit cell will contract, leading to an increase in force constants and consequently the frequencies are slightly higher in solid state. However, closer examination of the spectra of [EMIM][NO_3] reveals that most of bands move toward lower wave numbers when the liquid-solid phase transition occur. Owing to the influence of other factors such as hydrogen bonds and structural change, the frequency shift becomes more complicated. As to the bands at 1040.6 cm^{-1}, corresponding to symmetrical stretching vibration of [NO_3] anion, though propylammonium nitrate ([$C_3H_7NH_3$][NO_3]) samples also display polymorphism under lower temperature, there is split of the Raman band corresponding to the [NO_3] anion when the phase transition occurs, which is different with [EMIM][NO_3] [16]. These performances are intrinsically linked to the different reorganization of the hydrogen bonds.

The phase transitions are very sensitive to the conformational changes. Russina et al. has proposed that the changes are necessary (but not sufficient) step for the liquid to crystal transition [14]. The structure of cation [EMIM] has conformational equilibria for the CNCC angle and the full geometry optimizations indicate that the two conformers are planar and nonplanar ethyl groups against the imidazolium ring plane. The spectral range of 320–500 cm^{-1} of the Raman spectra is a better fingerprint for the cation [EMIM], where the bands at 387 cm^{-1}, 430 cm^{-1} and 448 cm^{-1} are assigned to the nonplanar, nonplanar, and planar conformers, respectively [27,28]. Fig. 4 shows that two conformers coexist in the liquid state, which is consistent with other reported ionic liquids, such as [EMIM][TFSI], [EMIM][CF_3SO_3] and [EMIM][BF_4] [27]. Nevertheless the band at 448 cm^{-1} almost disappears when the temperature decrease below 240 K. These changes of Raman bands evidence that this solid phase is composed mainly of nonplanar conformer, in agreement with the known [EMIM]Br crystal structure [28]. The mixture of [EMIM] conformers is established again just as the sample is heated to 300 K.

To further discuss the factor that affects the conformational stabilities of the cation [EMIM] at low temperature, enthalpy of the conformational change from nonplanar to planar ΔH° can be calculated on the basis of the relative intensities of the two conformers (I_p/I_{np}) dependence of the temperature by the following equation [27,28]:

$$-\mathrm{Ln}\left(\frac{I_p}{I_{np}}\right) = \frac{\Delta H^\circ}{RT} - \frac{\Delta S^\circ}{R} - \mathrm{Ln}\left(\frac{J_p}{J_{np}}\right)$$

Here R and T are the gas constant, absolute temperature, respectively. ΔS° denotes the entropy of the conformational change. J is the Raman scattering coefficient of the conformers, and subscripts *np* and *p* indicate nonplanar and planar conformers. The Ln (I_p/I_{np}) is plotted against 1/T temperature as shown in Fig. 4(b). By linear fitting the experimental data, the slope is 0.25 (I_{448}/I_{387}) and 0.46 (I_{448}/I_{430}). The ΔH° values obtained from the slope are 2.0 (I_{448}/I_{387}) and 3.8 kJ/mol (I_{448}/I_{430}), respectively. It is in agreement with the previous studies (3±1 kJ mol^{-1}) [27]. And the results further indicate that the nonplanar conformer is more stable at lower temperature, independent of the anion species in the liquid state.

In summary, Raman results show that the liquid [EMIM][NO_3] crystallize at 240 K, when the temperature is decreased to 180 K with cooling rate of 10 K/min. While the temperature is increased, it displays a continuous melting process, which has been assigned to structural modifications between polar and nonpolar domains. Phase transitions are closely linked with conformation change of the cation [EMIM] and reorganization of the hydrogen bonds.

For the compression process, Raman spectra with increasing pressure up to 4.5 GPa are illustrated in Fig. 5. As the sample is compressed, Raman spectra of [EMIM][NO_3] do not change as the increasing pressure up to 0. 9 GPa. The spectra exhibit significant changes as the pressure is elevated to 0.9 GPa. It can be seen that all Raman spectra become more intense and sharper, and some new bands emerge. According to the photomicrographs, the sample change gradually from a transparent liquid into a translucent solid.

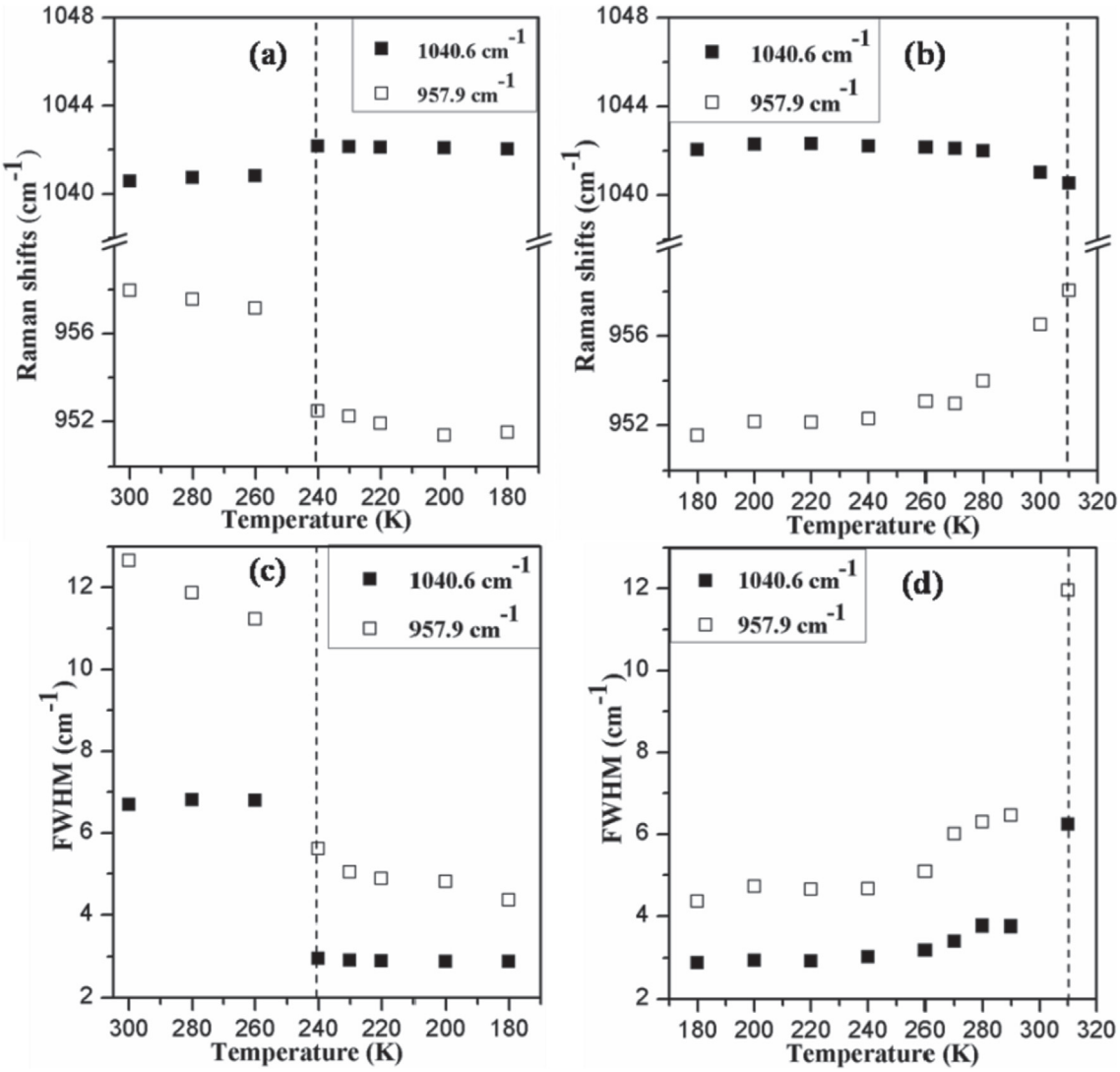

Fig. 3. Changes in (a) Raman shifts and (b) FWHM of $\nu_{str}(CC)$, $\nu_{ss}(NO_3)$ as a function of temperature. The vertical dashed lines represent the temperature of phase transition.

It is assumed that the phase transition is from liquid to solid I. With further compression up to 2.2 GPa, some remarkable changes occur in the spectra. The major evidence is that the bands at 1059.4 cm^{-1} emerged abruptly, and a parasitic shoulder appeared at 1406.7 cm^{-1} at the same time. Additionally, the relative intensities of C—H stretching modes (marked with down arrow in Fig. 5) change obviously. These Raman-mode changes evidence solid I to solid II phase transition, and the pattern preserves to about 4.5 GPa.

To further illustrate the multiple phase transitions of the [EMIM][NO_3], Fig. 6 displays the changes in the Raman shifts and FWHM of the characteristic spectrum as function of pressure. From Fig. 6(a), it can be seen that, with increasing pressure, all the observed modes shift linearly except two sudden changes in the slope of the frequency-pressure curves of some modes at about 0.9 GPa and 2.2 GPa. All of the Raman bands in this internal region exhibit shifts toward to the high frequencies owing to the decrease in the bond distance and increase in the effective force constants. The above results indicate that two structural transformations of [EMIM][NO_3] occur at about 0.9 GPa and 2.2 GPa respectively. These behaviors are consistent with the previous literature [18,19]. Owing to the vibrational relaxation by the molecular interactions under the high pressure, FWHM displays the pressure sensitive dependence. As shown from Fig. 6(b), the FWHM clearly change at each phase transition point mentioned and have larger half widths in the liquid and solid I. However, the smaller half widths are in solid II. These results suggest that [EMIM][NO_3] has free rotations in the liquid and solid I, while solid II is more orderly than the solid I.

The pressure-induced spectral changes in the lattice vibrational region due to the cation [EMIM] are plotted in Fig. 7(a) and Fig. 7(b). According to previous studies, the populations of conformer are proportional to specific band intensities. It was found the trends of these two Raman spectra 387 and 430 cm^{-1} are consistent [29]. Therefore only the intensity of 430 cm^{-1} and 448 cm^{-1} are used to evaluate the change of conformer populations in this ionic liquid. The intensity fractions (f) is defined as

$$f_{np} = \frac{I_{430}}{I_{448} + I_{430}}, \quad f_p = \frac{I_{448}}{I_{448} + I_{430}}$$

Here I_{430} and I_{448} indicate the Raman intensity of nonplanar and planar conformers of [EMIM], respectively. As shown in Fig. 7 (b), it can be seen that the intensity of the nonplanar initially gradually decrease with increasing pressure up to 0.9 GPa, and then decrease abruptly under the pressure above 0.9 GPa. As the sample is further compressed to 2.2 GPa, the planar conformer become dominant

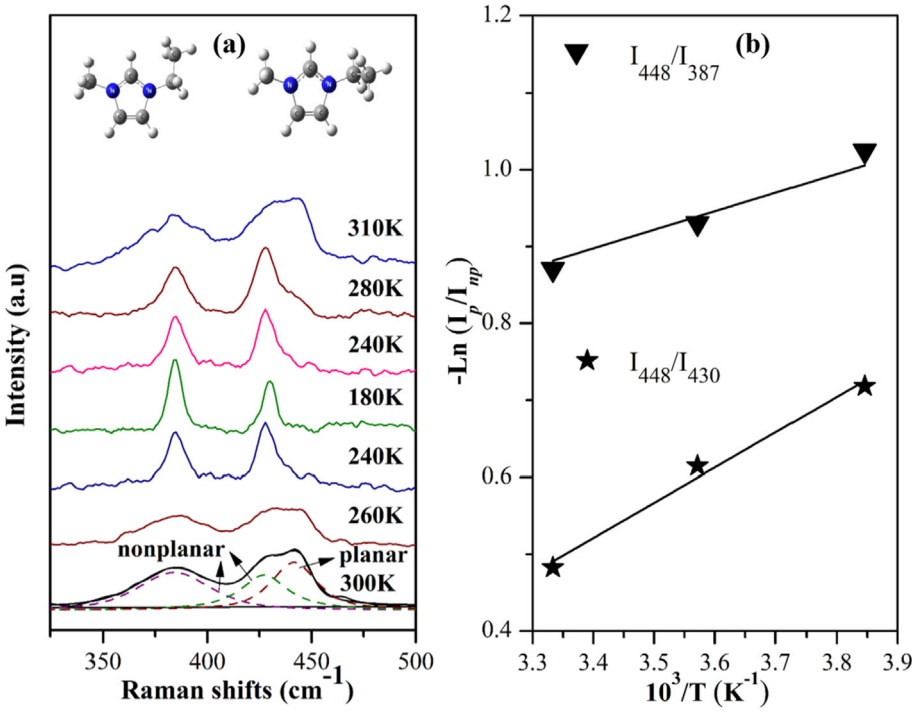

Fig. 4. (a) Raman spectral of [EMIM][NO_3] corresponding to the ranges 320–500 cm^{-1} at different temperatures. (b) Experimental and fitted plots of −Ln (I_p/I_{np}) versus inverse absolute temperature (1/T) in the range of 260–300 K.

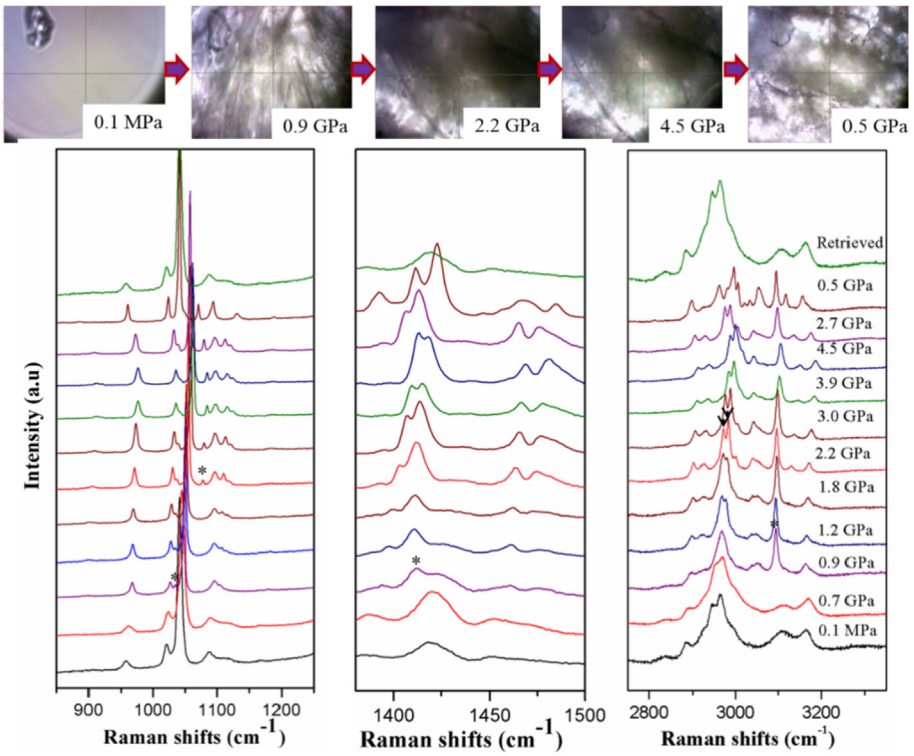

Fig. 5. Raman spectra of [EMIM][NO_3] at different pressure. Upper: Photomicrographs in the sample chamber of DAC at the room temperature under high pressures. The asterisks (*) represent new Raman peaks. The arrows indicate the changes in relative intensity of the two peaks.

and the contribution of nonplanar conformer is negligible. The planar conformer of [EMIM] also became predominant in the cation [EMIM] at high pressures, as discussed previously [20]. This experiment further illustrates that the phase transition of ILs are closely relevant with the conformational changes.

In addition, the volume difference (ΔV) between these two conformers can be determined by

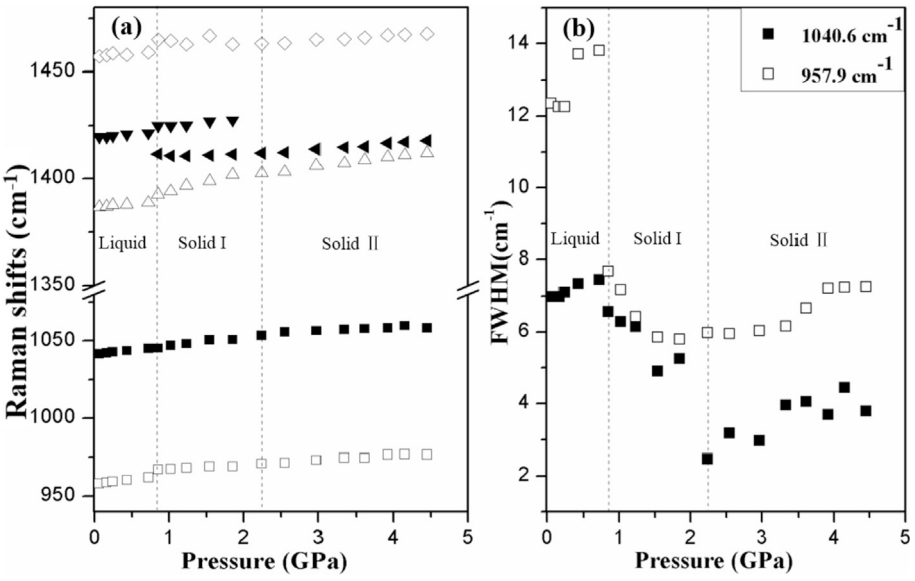

Fig. 6. Changes in (a) Raman shifts and (b) FWHM of ν_{str} (CC), ν_{ss} (NO3) as a function of pressure. The vertical dashed lines represent the pressure of phase transitions.

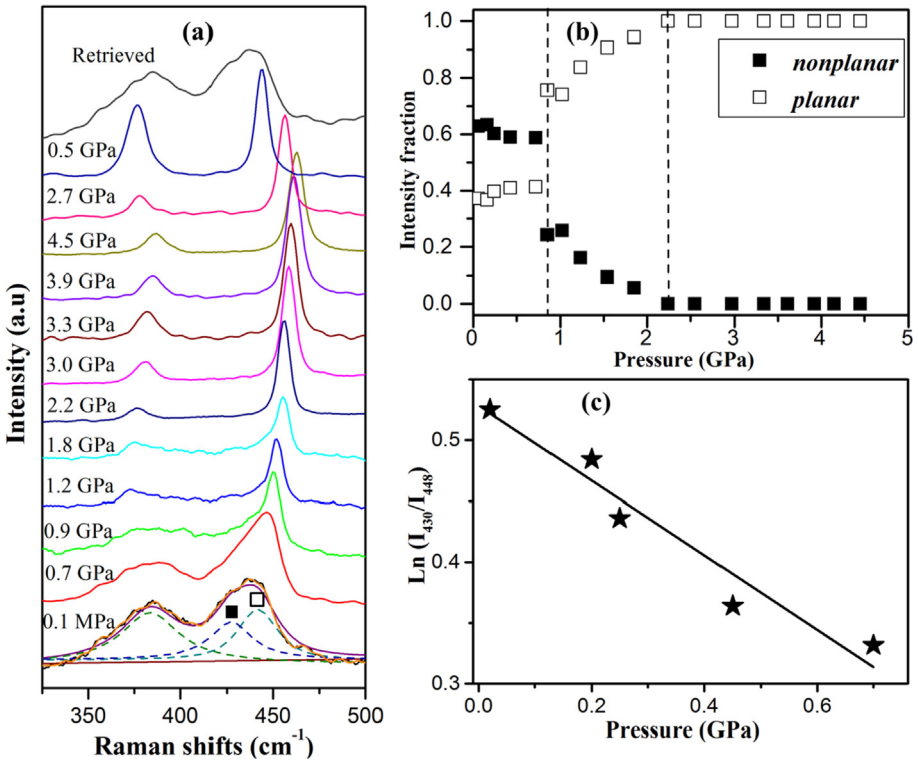

Fig. 7. (a) Raman spectral changes of [EMIM][NO_3] in the region from 320 to 500 cm^{-1}. (b) Intensity fractions of the conformers of [EMIM][NO_3] as a function of pressure. The open and closed squares represent the intensity fraction of the planar and nonplanar conformers, respectively. The vertical dashed lines represent the pressure of phase transitions. (c) Experimental and fitted plots of ln(I_{430}/I_{448}) as a function of pressure in the liquid state.

$$\Delta V^{p\rightarrow np} = -RT\left\{\frac{\partial \ln(I_{430}/I_{448})}{\partial P}\right\}$$

where *R*, *T*, *P* are the gas constant, ambient temperature (300 K in this experience) and pressure, respectively [11,29]. By using the slope obtained by linear fitting of the graph of ln (I_{430}/I_{448}) versus pressure in Fig. 7(c), the volume difference ΔV is determined to be 0.75 ± 0.17 cm^3/mol. This value is smaller than 1.6 ± 0.1 cm^3/mol for 1-ethyl-3-methylimidazolium tetrafluoroborate ([EMIM][BF_4]) and may be related to the type of anion [29]. The result indicates the planar conformer has a smaller molecular value, and the population of conformer with the lowest molecular volume increases as the pressure increases.

The Raman spectra of [EMIM][NO_3] have also been depicted upon decompression. As shown in Fig. 5, Raman spectroscopy has

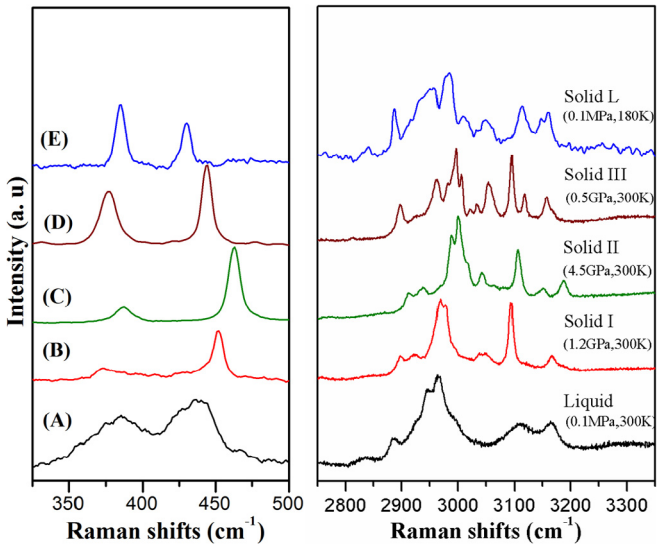

Fig. 8. Comparison of the Raman spectra of [EMIM][NO_3] at various states. (A) is the liquid state, (B) is the solid I, (C) is the solid II, (D) is the solid III, (E) is the solid L directly crystallized by cooling the sample below its melting point.

changed dramatically by decreasing pressure until ~0.5 GPa. There is a new phase transition (designated as solid III), which is quite different from solid I and solid II. While the solid III shows planar conformer either. It has been reported that two conformers coexist in the super-pressurized glass state, but the intensity of planar conformer is predominant [20,29]. There is only a planar conformation in the solid phase induced by high pressure. A new conformation would emerge, which is related with compression rate and the value of pressure [18,30]. However, conformational equilibrium under the solid phase induced by decompression is correlates with the anion structure which is believed to be due to cation-anion coulombic attraction and hydrogen bond [29,30]. The Raman spectra retrieved to ambient pressure are similar with those of the starting liquid phase, indicating that all the observed structural changes induced by compression is reversible.

According to the above discussion, there are one low temperature phase (solid L) and three high pressure phases (solid I, solid II and solid III) for [EMIM][NO_3]. The corresponding Raman spectra are displayed to compare different structure in the same Fig. 8. The spectra of high pressure phase is distinct from that of low temperature solid L, which indicate that there are large distinctions in the phase behavior responding to the external conditions (low temperature or high pressure). The temperature only produces a simultaneous change in the thermal energy and the volume, while pressure can change the intermolecular interactions without encountering major perturbations, therefore, the effect of pressure on the vibration frequency and Raman shape is usually larger than the temperature [31]. It may be a cause for the difference in phase behavior under different external condition such as low temperature and high pressure.

4. Summary

In summary, phase transitions and polymorphs of [EMIM][NO_3] have been studied in detail by using DSC and Raman technology. DSC result indicates that ionic liquid [EMIM][NO_3] undergoes the first order phase transition near 251 K upon cooling. Upon heating, there is a pre-melting process over a wide temperature range and the melting point is about 289 K. Detailed temperature-dependent Raman data also shows most of Raman spectra experience obviously shifting and narrowing at about 240 K which is attributed to the first-order phase transition. The liquid-solid phase transition is associated with the change of cation conformation from nonplanar-planar equilibrium in the liquid to planar in the solid L. High-pressure Raman studies of ionic liquid [EMIM][NO_3] reveals that the liquid to solid I transition takes place at about 0.9 GPa, while the solid I to solid II transition occurs at about 2.2 GPa. The solid phase II is more orderly than the solid phase I. The third transition is induced by releasing pressure to ~0.5 GPa. The nonplanar conformer of cation [EMIM] becomes predominant in solid I phase and there is only nonplanar conformer in solid II and solid III. Finally, the phase transition upon low temperature or high pressure is fully reversible. The present study will enhance a better understanding of solidification of this class of compounds.

Acknowledgments

This work is supported by the National Natural Science Foundation of China (No. 11404292), Key Research Project of Higher Education of Henan Province (No. 18B140013) and Research and Practice Projects of Higher Education Teaching Reform of Henan Province (No. 2017SJGLX356).

References

[1] R.D. Rogers, K.R. Seddon, Science 302 (2003) 792.
[2] A.V. Mudring, Aust. J. Chem. 63 (2010) 544.
[3] F.M. Vitucci, D. Manzo, M.A. Navarra, O. Palumbo, F. Trequattrini, S. Panero, P. Bruni, F. Croce, A. Paolone, J. Phys. Chem. C 118 (2012) 5749.
[4] A. Efimova, G. Hubrig, P. Schmidt, Thermochim. Acta 573 (2013) 162.
[5] E. Gómez, N. Calvar, Domínguez ángeles, A. Macedo Eugénia, Fluid Phase Equilib. 470 (2018) 51.
[6] M. Imanari, K. Fujii, T. Mukai, N. Mizushima, H. Seki, K. Nishikawa, Physiol. Chem. Phys. 17 (2015) 8750.
[7] Y. Shimizu, K. Fuji, M. Imanari, K. Nishikawa, J. Phys. Chem. B 119 (2015) 12552.
[8] P.B.P. Serra, F.M.S. Ribeiro, M.A.A. Rocha, M. Fulem, K. Ruzicka, L.M.N.B.F. Santos, J. Chem. Thrmodyn. 100 (2016) 124.
[9] L.F.O. Faria, T.A. Lima, F.F. Ferreira, M.C.C. Ribeiro, J. Phys. Chem. B 122 (2018) 1972.
[10] X.R. Cheng, Y.Y. Li, J.M. Shang, C.S. Hu, Y.F. Ren, M. Liu, Z.M. Qi, Nano Res. 11 (2018) 855.
[11] F. Capitani, F. Trequattrini, O. Palumbo, A. Paolone, P. Postorino, J. Phys. Chem. B 120 (2016) 2921.
[12] T.A. Lima, V.H. Paschoal, L.F.O. Faria, M.C.C. Ribeiro, F.F. Ferreira, F.N. Costa, C. Giles, J. Phys. Chem. 144 (1) (2016) 224505.
[13] X. Zhu, H.N. Li, Z. Wang, C.S. Yuan, P.W. Zhu, L. Su, K. Yang, J. Wu, G.Q. Yang, X.D. Lie, RSC Adv. 7 (2017) 26428.
[14] O. Russina, B. Fazio, C. Schmidt, A. Triolo, Physiol. Chem. Phys. 13 (2011) 12067.
[15] S. Saouane, S.E. Norman, C. Hardacre, F.P.A. Fabbiani, Chem. Sci. 4 (2013) 1270.
[16] L.F. Faria, T.C. Penna, M.C. Ribeiro, J. Phys. Chem. B 117 (2013) 10905.
[17] M. Sobota, V. Dohnal, P. Vrbka, J. Phys. Chem. B 113 (2009) 4323.
[18] Y. Yoshimura, T. Takekiyo, H. Abe, N. Hamaya, J. Mol. Liq. 206 (2015) 89.
[19] H. Abe, T. Takekiyo, Y. Yoshimura, N. Hamaya, S. Ozawa, Aust. J. Chem. 72 (2019) 87.
[20] Y. Yoshimura, H. Abe, T. Takekiyo, M. Shigemi, N. Hamaya, R. Wada, M. Kato, J. Phys. Chem. B 117 (2013) 12296.
[21] L.F. Faria, T.A. Lima, M.C. Ribeiro, Cryst. Growth Des. 17 (2017) 5384.
[22] H.K. Mao, Science 200 (1978) 1145.
[23] J.S. Wilkes, M.J. Zaworotko, ChemInform 23 (1992) 965.
[24] L.F. Faria, J.R. Matos, M.C. Ribeiro, J. Phys. Chem. B 116 (2012) 9238.
[25] J. Kiefer, J. Fries, A. Leipertz, Appl. Spectrosc. 61 (2007) 1306.
[26] H.C. Chang, J.C. Jiang, J.C. Su, C.Y. Chang, S.H. Lin, J. Phys. Chem. 111 (2007) 9201.
[27] Y. Umebayashi, T. Fujimori, T. Sukizaki, M. Asada, K. Fujii, R. Kanzaki, S. Ishiguro, J. Phys. Chem. 109 (2005) 8976.
[28] J.C. Lassegues, J. Grondin, R. Holomb, P. Johansson, J. Raman Spectrosc. 38 (2007) 551.
[29] Y. Imai, T. Takekiyo, N. Hatano, H. Abe, Y. Yoshimura, Chem. Phys. Lett. 511 (2011) 241.
[30] H.N. Li, Z. Wang, L.C. Chen, J. Wu, H.J. Huang, K. Yang, Y.Q. Wang, L. Su, G.Q. Yang, J. Phys. Chem. B 119 (2015) 14245.
[31] T.C. Penna, L.F. Faria, J.R. Matos, M.C. Ribeiro, J. Phys. Chem. 138 (1) (2013) 104503.